GDCh Communications Angewandte International Edition Chemie

Siliconoids Hot Paper

How to cite: Angew. Chem. Int. Ed. **2020**, 59, 8532–8536
International Edition: doi.org/10.1002/anie.202001178
German Edition: doi.org/10.1002/ange.202001178

Indirect and Direct Grafting of Transition Metals to Siliconoids

*Nadine E. Poitiers, Luisa Giarrana, Kinga I. Leszczyńska, Volker Huch, Michael Zimmer, and David Scheschkewitz**

Dedicated to Professor Reinhold Tacke on the occasion of his 70th birthday

***Abstract:** Unsaturated charge-neutral silicon clusters (siliconoids) are important as gas-phase intermediates between molecules and the elemental bulk. With stable zirconocene- and hafnocene-substituted derivatives, we here report the first examples containing directly bonded transition-metal fragments that are readily accessible from the ligato-lithiated Si$_6$ siliconoid (**1Li**) and Cp$_2$MCl$_2$ (M = Zr, Hf). Charge-neutral siliconoid ligands with pending tetrylene functionality were prepared by the reaction of amidinato chloro tetrylenes [PhC(NtBu)$_2$]ECl (E = Si, Ge, Sn) with **1Li**, thus confirming the principal compatibility of such low-valent functionalities with the unsaturated Si$_6$ cluster scaffold. The pronounced donor properties of the tetrylene/siliconoid hybrids allow for their coordination to the Fe(CO)$_4$ fragment.*

The synthesis of stable unsaturated silicon clusters (siliconoids)[1] has attracted considerable interest because of the presumed intermediacy of the parent species in gas-phase deposition processes[2] as well as the fact that the unsubstituted vertices are reminiscent of the free valencies of bulk and nano silicon surfaces.[3] Since the report of the first stable siliconoid,[4] a variety of further examples have been prepared by the groups of Wiberg,[5] Kyushin,[6] Iwamoto,[7] Breher,[8] Fässler,[9] Lips,[10] and our group.[11] The two recent syntheses of regioisomeric lithiated Si$_6$ siliconoids (benzpolarenes)[11d,f] and their facile functionalization with suitable electrophiles considerably enlarged the scope of this emerging field towards the related Zintl anions (polyanionic, deltahedral clusters without any substituents). The presence of organic substituents in siliconoids confers higher solubility, while the electronic properties are retained as manifest in the wide dispersion of ^{29}Si NMR shifts.[4,6,8,11,12] While Zintl anions of Group 14 elements heavier than silicon have been frequently applied in the synthesis of partially substituted metalloid clusters,[13] the grafting of substituents to silicon-based Zintl anions has only been achieved very recently by the groups of Korber[14] and Fässler,[15] who independently reported the protonation of silicon Zintl anions to the partially H-substituted anionic clusters [HSi$_9$]$^{3-}$, [H$_2$Si$_9$]$^{2-}$, and [HSi$_4$]$^{3-}$.[16] In addition, the Fässler group successfully transferred silyl substituents to Si$_9$$^{4-}$.[9]

Zintl silicide anions have been employed as extraordinarily electron-rich ligands towards transition-metal centers.[17] Conversely, the coordination of neutral siliconoids to metals has thus far remained elusive. Here, with zirconocene and hafnocene derivatives, we report the first examples of siliconoids bearing covalently attached transition-metal functionalities. As attempts to coordinate charge-neutral siliconoids to transition-metal fragments in a dative manner remained inconclusive, we resorted to the grafting of amidinato tetrylene residues PhC(N*t*Bu)$_2$E (E = Si, Ge, Sn)[18–20] to the Si$_6$ scaffold. Given that tetrel(II) species are well established as ligands in catalysis,[21] it was conceivable that tetrylene functionalization would facilitate the coordination of electron-rich siliconoid moieties to transition-metal centers. As will be elaborated further on, the targeted tetrylene–siliconoid hybrids are stable and indeed readily transformed into the corresponding Fe(CO)$_4$ complexes.

Treatment of Cp$_2$MCl$_2$ (M = Zr, Hf) with the *ligato*-lithiated siliconoid **1Li** results in rapid and uniform conversion into the corresponding Group 4 metalated siliconoids **2a** and **2b** (Scheme 1). In contrast, reaction with one equivalent of titanocene dichloride led to a complicated mixture of products, presumably because of competing redox reactions. The diagnostically wide dispersion of ^{29}Si signals confirmed the presence of uncompromised benzpolarene scaffolds.[11d,f] The signals of the *privo*-silicon atoms appear at the usual low field at 162.6 (**2a**) and 162.8 ppm (**2b**), while the two unsubstituted *nudo*-vertices give rise to two individual signals

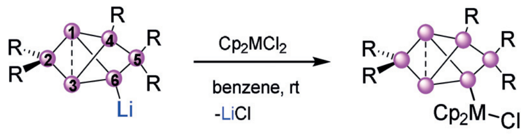

1 **2a,b**

Scheme 1. Synthesis of *ligato*-metallocene-substituted Si$_6$ siliconoids **2a** and **2b**. **2a**: M = Zr; **2b**: M = Hf. Tip = triisopropylphenyl. The "naked" positions 1 and 3 are referred to as *nudo*, the NMR-deshielded position 2 as *privo*, the mono-substituted positions 4 and 6 as *ligato*, and the remote position 5 as *remoto*.[11f]

---

[*] N. E. Poitiers, L. Giarrana, Dr. K. I. Leszczyńska, Dr. V. Huch, Dr. M. Zimmer, Prof. Dr. D. Scheschkewitz
Krupp-Chair of Inorganic and General Chemistry
Saarland University
Campus Saarbrücken C4.1, 66123 Saarbrücken (Germany)
E-mail: scheschkewitz@mx.uni-saarland.de

Supporting information and the ORCID identification number(s) for the author(s) of this article can be found under: https://doi.org/10.1002/anie.202001178.

Table 1: Selected analytical data of metallocene-substituted siliconoids **2a** and **2b**.

	δ(^{29}Si2) [ppm]	δ(^{29}Si1/3) [ppm]	Si1–Si3 [Å]	Si4–M [Å], exp	Si4–M [Å], calc	λ_{max} [nm]
2a (M = Zr)	162.6	−233.5 −240.6	2.588(2)	2.782(1)	2.741	521
2b (M = Hf)	162.8	−232.1 −240.3	2.588(1)	2.770(1)	2.738	497

at characteristically high field at −233.5 and −240.6 ppm for **2a** and −232.1 and −240.3 ppm for **2b** (Table 1). The apparent symmetry reduction is typical for *ligato*-substituted benzpolarenes and has been attributed to hindered rotation of the pending functionality.[11d] The other ^{29}Si NMR chemical shifts are located within the usual range for saturated silicon atoms and vary only slightly with the introduced ligand (see the Supporting Information).

The longest-wavelength absorptions in the UV/Vis spectra are at $\lambda_{max} = 521$ nm (**2a**) and 497 nm (**2b**), and therefore slightly red-shifted in comparison with previously reported *ligato*-substituted siliconoids ($\lambda_{max} = 364$–477 nm).[11d,f] Single crystals were obtained by crystallization from hexane/toluene in 53% (**2a**) and 66% (**2b**) yield, and their structures were confirmed by X-ray diffraction in the solid state (Figure 1).

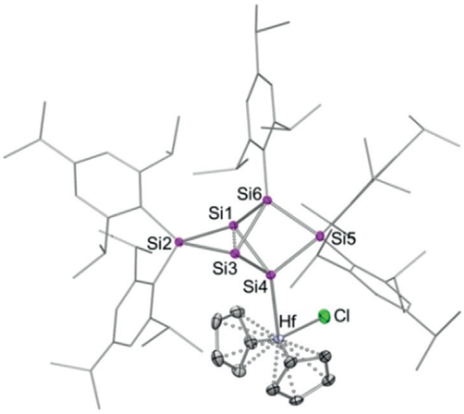

Figure 1. Representative molecular structure of siliconoid **2b** in the solid state.[30] Hydrogen atoms omitted for clarity. Thermal ellipsoids set at 50% probability. For the structure of **2a**, see the Supporting Information.

The distances between the unsubstituted bridgehead silicon atoms Si1 and Si3 (**2a**: 2.588(2) Å; **2b**: 2.588(1) Å) are significantly shorter than those of the peraryl-substituted global-minimum isomer[11b] and in line with previously reported persilabenzpolarenes with electropositive groups in the *ligato*-position.[11d,f] The electronic nature of the substituent apparently affects the electron density available for cluster bonding.

The Zr–Si bond length of 2.782(1) Å in **2a** is in between that reported for a disilenyl-substituted zirconocene chloride on the one hand (2.7611 Å)[22c] and silyl-substituted zirconocene complexes on the other hand (2.813–2.8214 Å).[22] Similarly, the Hf–Si bond of 2.7702(9) Å in **2b** is shorter than those reported for tetracoordinated hafnium compounds (2.835–2.888 Å).[23] The experimental bond lengths were satisfyingly reproduced by DFT calculations for **2a** and **2b** at the BP86 + D3(BJ)/def2-SVP level of theory (Table 1).

In solution, even smallest traces of water lead to the progressive hydrolysis of *ligato*-zirconocene-functionalized siliconoid **2a** as indicated by the gradual appearance of a second set of signals, including a characteristic Si–H resonance at 4.103 ppm, in the ^{1}H NMR spectrum.[22c] The Si–Hf bond of *ligato*-hafnocene-functionalized siliconoid **2b** exhibits a considerably higher stability towards hydrolysis (see the Supporting Information for details). In view of the instability of the covalent silicon–metal bond in **2a** and **2b**, it is unsurprising that attempts to directly graft later transition metals to siliconoids have failed thus far. In the same vein, the dative coordination of charge-neutral siliconoids to transition metals is also unknown. We therefore considered the functionalization of the Si_6 scaffold with an auxiliary tetrylene ligand in order to facilitate coordination.

Tetrylenes are known for their excellent σ-donating properties. As the reaction of *ligato*-lithiated benzpolarene **1Li** with Jutzi's silicocene affords the cluster-expanded Si_7 siliconoid[11e] instead of the simple substitution product, we chose the N-heterocyclic chloro tetrylenes of the Roesky type in the expectation that the nitrogen donors adjacent to the Si^{II} center would tame its electron deficiency sufficiently to allow for the isolation of a silylene-functionalized Si_6 siliconoid. In fact, the tetrylenes $[PhC(NtBu)_2]ECl$ are known to readily undergo nucleophilic substitution of the chlorine substituent.[19] Treatment of the *ligato*-lithiated benzpolarene **1Li** with 1.1 equivalents of $[PhC(NtBu)_2]ECl$[19,20] indeed leads to rapid conversion into uniform products (E = Si, Ge, Sn; Scheme 2) accompanied by precipitation of LiCl. ^{29}Si NMR analysis showed the diagnostic wide dispersion of chemical shifts (as discussed above for **2a** and **2b**), and thus confirmed the anticipated integrity of the benzpolarene scaffolds suggesting the formation of siliconoids **3a–c**. An additional signal in the ^{29}Si NMR spectrum of **3a** was assigned to the pending silylene center.[20a,c]

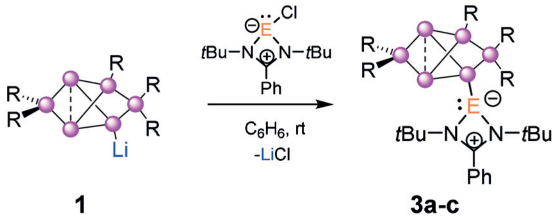

Scheme 2. Synthesis of the tetrylene-functionalized Si_6 siliconoids **3a–c**. **3a**: E = Si; **3b**: E = Ge; **3c**: E = Sn.

The occurrence of two sets of signals each in the ^{29}Si and ^{119}Sn NMR spectra of **3b** and **3c** suggested the presence of rotational isomers in solution. Indeed, ^{29}Si and ^{119}Sn solid-state NMR spectra of **3a–c** show just a single set of signals (Table 2 and the Supporting Information). A VT-NMR study

Table 2: Selected NMR shifts of the tetrylene-functionalized siliconoids **3a**–**c**.

	$\delta(^{29}Si2)$ [ppm]	$\delta(^{29}Si1/3)$ [ppm]	$\delta(^{29}Si2)$ solid [ppm]	$\delta(^{29}Si1/3)$ solid [ppm]	$\delta(^{119}Sn)$ [ppm]	$\delta(^{119}Sn)$ solid [ppm]
3a	166.7	−244.6 −260.7	160.0	−250.5 −262.6	–	–
3b major	167.3	−245.4 −261.1	163.4	−248.9 −261.2	–	–
3b minor	165.6	−233.9 −238.1	–	–	–	–
3c major	162.3	−232.6 −236.9	–	–	267.8	–
3c minor	168.8	−242.3 −259.3	162.9	−244.3 −259.9	336.5	332.0

in toluene solution revealed the onset of coalescence at 343 K for germylene-substituted **3b** although the barrier proved to be too high to allow for accurate determination of the coalescence temperature (> 70 °C). The ^{29}Si and ^{1}H NMR spectra of stannylene-substituted **3c** show broad signals with poor signal-to-noise ratios at room temperature, suggesting that the coalescence temperature may be within reach. Accordingly, VT-NMR analysis of **3c** at low temperature (226 K) revealed sharpened signals in the ^{1}H NMR spectrum as well as a second set of less intense signals in the ^{29}Si NMR spectrum (Table 2).

The longest-wavelength absorption bands in the UV/Vis spectra are at $\lambda_{max} = 472$ nm (**3a**), 436 nm (**3b**), and 436 nm (**3c**). Single crystals were obtained in 72 % (**3a**), 78 % (**3b**), and 74 % (**3c**) yield, and the structures were confirmed by X-ray diffraction studies (Figure 2). The structure of the Si_6 cluster core is hardly influenced by the nature of the tetrylene ligand. The distances between the unsubstituted bridgehead silicon atoms Si1 and Si3 (**3a**: 2.6039(9) Å; **3b**: 2.612(2) Å; **3c**: 2.6149(8) Å) are slightly shorter than in the global-minimum isomer Si_6Tip_6[11b] and in line with previously reported *ligato*-functionalized siliconoids with electropositive groups.[11d,f] The bonds between Si4 and the pending tetrylene (**3a**: 2.4294(9) Å; **3b**: 2.493(2) Å; **3c**: 2.6753(6) Å) are longer than typical single bonds.[24–27]

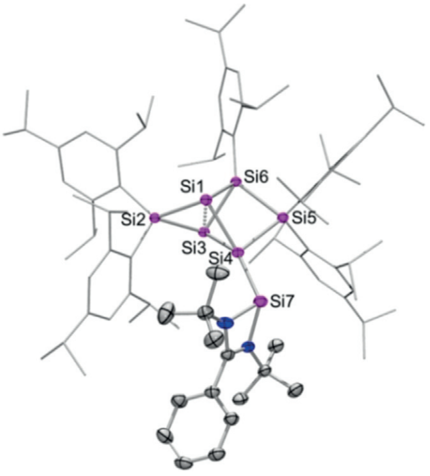

Figure 2. Representative molecular structure of silylene-functionalized siliconoid **3a** in the solid state.[30] Hydrogen atoms omitted for clarity. Thermal ellipsoids set at 50 % probability. For the structures of **3b** and **3c**, see the Supporting Information.

In order to probe the suitability of **3a**–**c** as neutral ligands towards transition metals, we attempted the coordination to $Fe(CO)_4$ in a proof-of-principle study (Scheme 3). Complexes **4a**–**c** are obtained in a straightforward manner by stirring a benzene solution of **3a**–**c** with 4 (**4a**), 5 (**4b**), or 1.5 (**4c**) equivalents of $Fe_2(CO)_9$[18,19a,28] at room temperature. Complexes **4a**–**c** were fully characterized by X-ray diffraction on single crystals, elemental analysis, as well as multinuclear NMR, UV/Vis, and IR spectroscopy.

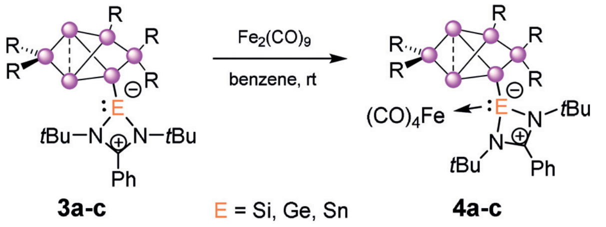

Scheme 3. Reaction of the tetrylene-functionalized Si_6 siliconoids **3a**–**c** with $Fe_2(CO)_9$ to afford the corresponding $Fe(CO)_4$ complexes **4a**–**c**.

The ^{29}Si NMR spectra of **4a**–**c** show a similarly wide distribution in chemical shifts as those of **3a**–**c**, albeit with distinctly different numerical values. In the ^{29}Si NMR spectrum, the additional signal of the silylene moiety of **4a** at 110.0 ppm is drastically downfield-shifted compared to that of **3a** (48.0 ppm). Similarly, the stannylene side arm of **4c** shows a ^{119}Sn NMR signal at 456.3 ppm (Table 3). A related LSnCl–$Fe(CO)_4$ complex resonates at much higher field at 255 ppm.[19a] ^{1}H and ^{13}C NMR analyses of **4a**–**c** in C_6D_6 confirmed the presence of two singlet resonances each assignable to the *tert*-butyl groups.

According to the UV/Vis spectra of **4a**–**c**, the longest-wavelength absorption bands are observed at $\lambda_{max} = 470$ nm (**4a**), 469 nm (**4b**), 466 nm (**4c**) and thus slightly blue-shifted compared to those of **3a**–**c**. The $Fe(CO)_4$ complexes **4a**–**c** exhibit IR characteristics of tetrylene–$Fe(CO)_4$ complex-

Table 3: Selected NMR shifts of $Fe(CO)_4$ complexes of tetrylene-substituted siliconoids **4a**–**c**.

	$\delta(^{29}Si2)$ [ppm]	$\delta(^{29}Si1/3)$ [ppm]	$\delta(^{29}Si2)$ solid [ppm]	$\delta(^{29}Si1/3)$ solid [ppm]	$\delta(^{119}Sn)$ [ppm]	$\delta(^{119}Sn_{CP/MAS})$ [ppm]
4a	165.1	−198.2 −230.4	158.2	−195.9 −231.2	–	–
4b	163.7	−203.0 −231.4	156.7	−202.2 −232.8	–	–
4c	160.2	−201.7 −230.7	154.1	−200.3 −232.8	456.3	469.2

es,[28a,29] with CO stretching modes at $\upsilon = 1899$, 1913, 1948, 2022 cm^{-1} (**4a**), 1908, 1918, 1949, 2025 cm^{-1} (**3b**), and 1902, 1914, 1942, 2015 cm^{-1} (**4c**). The donor strength of **4a–c** can be classified by the asymmetric carbonyl absorptions at $\upsilon = 2022\ cm^{-1}$ (**4a**), 2025 cm^{-1} (**4b**), and 2015 cm^{-1} (**4c**), which indicate a slightly lower ligand-to-metal σ-donation compared to other tetrylene $Fe(CO)_4$ complexes such as $\{[PhC(NtBu)_2]SiOtBu\}Fe(CO)_4$ ($\upsilon = 2026\ cm^{-1}$)[28a] and $\{[PhC(NtBu)_2]GeCl\}Fe(CO)_4$ ($\upsilon = 2042\ cm^{-1}$).[28c] Single crystals of **4a–c** were obtained in 75% (**4a**), 60% (**4b**), and 70% (**4c**) yield, and the structures were confirmed to be isosteric by X-ray diffraction studies (Figure 3). The distances between the bridgehead silicon atoms Si1–Si3 (**4a**: 2.560(1) Å; **4b**: 2.566(1) Å; **4c**: 2.5756(7) Å) are slightly shorter than in **3a–c**. This is indicative of increased electron density within the cluster scaffold upon formation of the transition-metal complex. The bonds Si−E in **4a–c** (**4a**: 2.384(1) Å; **4b**: 2.4422(8) Å; **4c**: 2.5896(5) Å) are equally shortened compared to **3a–c** and now in the typical range of Si−E single bonds (E = Si, Ge, Sn).[24–27] The $Fe(CO)_4$ complexes **4a–c** exhibit typical Fe−E distances (**4a**: 2.279(1) Å; **4b**: 2.3496(5) Å; **4c**: 2.4957(3) Å).[18,19a,28a–c]

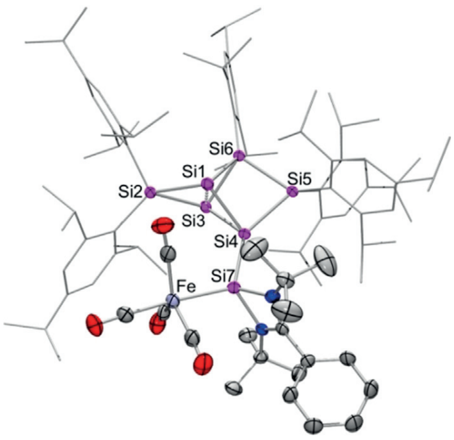

Figure 3. Representative molecular structure of the $Fe(CO)_4$ complex of **4a** in the solid state.[30] Hydrogen atoms omitted for clarity. Thermal ellipsoids set at 50% probability. For the structures of **4b** and **4c**, see the Supporting Information.

In conclusion, with **2a** and **2b**, we have reported the first transition-metal-substituted neutral siliconoids. The reaction of an anionic Si_6 siliconoid with $PhC(NtBu)_2ECl$ (E = Si, Ge, Sn) gave rise to siliconoids with pending Roesky-type silylene, germylene, and stannylene moieties, an unprecedented feature in silicon cluster chemistry. Unlike in the case of the previously attempted grafting of a Cp*-substituted silylene fragment,[11e] the electrophilicity of the tetrylenes of the Roesky type is sufficiently low, thereby avoiding the otherwise observed expansion of the cluster core. As proof of concept for the suitability of these novel ligands in the coordination to transition metals, we synthesized and characterized the corresponding $Fe(CO)_4$ complexes **4a–c**.

Acknowledgements

Funding by the Deutsche Forschungsgemeinschaft (DFG SCHE 906/4-1 and 4-2) is gratefully acknowledged. We thank Dr. Diego Andrada for helpful discussions and DFT calculations.

Conflict of interest

The authors declare no conflict of interest.

Keywords: clusters · ligands · low-valent species · silicon · siliconoids

---

[1] a) Y. Heider, D. Scheschkewitz, *Dalton Trans.* **2018**, *47*, 7104–7112; b) S. Kyushin in *Organosilicon Compounds: Theory and Experiment (Synthesis)*, *Vol. 1* (Ed.: V. Y. Lee), Academic Press, New York, **2017**, chap. 3; c) T. Iwamoto, S. Ishida, *Chem. Lett.* **2014**, *43*, 164–170; d) F. Breher, *Coord. Chem. Rev.* **2007**, *251*, 1007–1043.

[2] a) T. M. I. Davidson, *J. Organomet. Chem.* **1970**, *24*, 97–100; b) H. Murakami, T. Kanayama, *Appl. Phys. Lett.* **1995**, *67*, 2341–2343; c) M. Watanabe, H. Murakami, T. Miyazaki, T. Kanayama, *Appl. Phys. Lett.* **1997**, *71*, 1207–1209; d) W. M. M. Kessels, M. C. M. Van De Sanden, D. C. Schram, *Appl. Phys. Lett.* **1998**, *72*, 2397–2399; e) G. A. Rechtsteiner, O. Hampe, M. F. Jarrold, *J. Phys. Chem. B* **2001**, *105*, 4188–4194.

[3] H. Neergaard Waltenburg, J. T. Yates, Jr., *Chem. Rev.* **1995**, *95*, 1589–1673.

[4] D. Scheschkewitz, *Angew. Chem. Int. Ed.* **2005**, *44*, 2954–2956; *Angew. Chem.* **2005**, *117*, 3014–3016.

[5] G. Fischer, V. Huch, P. Mayer, S. K. Vasisht, M. Veith, N. Wiberg, *Angew. Chem. Int. Ed.* **2005**, *44*, 7884–7887; *Angew. Chem.* **2005**, *117*, 8096–8099.

[6] a) A. Tsurusaki, C. Iizuka, K. Otsuka, S. Kyushin, *J. Am. Chem. Soc.* **2013**, *135*, 16340–16343; b) A. Tsurusaki, J. Kamiyama, S. Kysushin, *J. Am. Chem. Soc.* **2014**, *136*, 12896–12898.

[7] T. Iwamoto, N. Akasaka, S. Ishida, *Nat. Commun.* **2014**, *5*, 5353.

[8] D. Nied, R. Köppe, W. Klopper, H. Schnöckel, F. Breher, *J. Am. Chem. Soc.* **2010**, *132*, 10264–10265.

[9] L. J. Schiegerl, A. J. Karttunen, W. Klein, T. F. Fässler, *Chem. Eur. J.* **2018**, *24*, 19171–19174.

[10] J. Keuter, K. Schwedtmann, A. Hepp, K. Bergander, O. Janka, C. Doerenkamp, H. Eckert, C. Mück-Lichtenfeld, F. Lips, *Angew. Chem. Int. Ed.* **2017**, *56*, 13866–13871; *Angew. Chem.* **2017**, *129*, 14054–14059.

[11] a) K. Abersfelder, A. J. P. White, H. S. Rzepa, D. Scheschkewitz, *Science* **2010**, *327*, 564–566; b) K. Abersfelder, A. J. P. White, R. J. F. Berger, H. S. Rzepa, D. Scheschkewitz, *Angew. Chem. Int. Ed.* **2011**, *50*, 7936–7939; *Angew. Chem.* **2011**, *123*, 8082–8086; c) A. Jana, V. Huch, M. Repisky, R. J. F. Berger, D. Scheschkewitz, *Angew. Chem. Int. Ed.* **2014**, *53*, 3514–3518; *Angew. Chem.* **2014**, *126*, 3583–3588; d) P. Willmes, K. Leszczyńska, Y. Heider, K. Abersfelder, M. Zimmer, V. Huch, D. Scheschkewitz, *Angew. Chem. Int. Ed.* **2016**, *55*, 2907–2910; *Angew. Chem.* **2016**, *128*, 2959–2963; e) K. I. Leszczyńska, V. Huch, C. Präsang, J. Schwabedissen, R. J. F. Berger, D. Scheschkewitz, *Angew. Chem. Int. Ed.* **2019**, *58*, 5124–5128; *Angew. Chem.* **2019**, *131*, 5178–5182; f) Y. Heider, N. E. Poitiers, P. Willmes, K. I. Leszczyńska, V. Huch, D. Scheschkewitz, *Chem. Sci.* **2019**, *10*, 4523–4530; g) L. Klemmer, V. Huch, A. Jana, D. Scheschkewitz, *Chem. Commun.* **2019**, *55*, 10100–10103.

[12] a) M. Moteki, S. Maeda, K. Ohno, *Organometallics* **2009**, *28*, 2218–2224; b) S. Ishida, K. Otsuka, Y. Toma, S. Kyushin, *Angew. Chem. Int. Ed.* **2013**, *52*, 2507–2510; *Angew. Chem.* **2013**, *125*, 2567–2570.

[13] a) S. C. Sevov, J. M. Goicoechea, *Organometallics* **2006**, *25*, 5678–5692; b) S. Scharfe, F. Kraus, S. Stegmaier, A. Schier, T. F. Fässler, *Angew. Chem. Int. Ed.* **2011**, *50*, 3630–3670; *Angew. Chem.* **2011**, *123*, 3712–3754; c) F. Li, A. Muñoz-Castro, S. C. Sevov, *Angew. Chem. Int. Ed.* **2012**, *51*, 8581–8584; *Angew. Chem.* **2012**, *124*, 8709–8712; d) F. Li, S. C. Sevov, *J. Am. Chem. Soc.* **2014**, *136*, 12056–12063; e) O. Kysliak, C. Schrenk, A. Schnepf, *Inorg. Chem.* **2015**, *54*, 7083–7088; f) O. Kysliak, A. Schnepf, *Dalton Trans.* **2016**, *45*, 2404–2408; g) F. S. Geitner, J. V. Dums, T. F. Fässler, *J. Am. Chem. Soc.* **2017**, *139*, 11933–11940; h) F. S. Geitner, W. Klein, T. F. Fässler, *Angew. Chem. Int. Ed.* **2018**, *57*, 14509–14513; *Angew. Chem.* **2018**, *130*, 14717–14721; i) S. Frischhut, W. Klein, M. Drees, T. F. Fässler, *Chem. Eur. J.* **2018**, *24*, 9009–9014.

[14] C. Lorenz, F. Hastreiter, K. Hioe, N. Lokesh, S. Gärtner, N. Korber, R. M. Gschwind, *Angew. Chem. Int. Ed.* **2018**, *57*, 12956–12960; *Angew. Chem.* **2018**, *130*, 13138–13142.

[15] T. Henneberger, W. Klein, T. F. Fässler, *Z. Anorg. Allg. Chem.* **2018**, *644*, 1018–1027.

[16] F. Hastreiter, C. Lorenz, J. Hioe, S. Gärtner, N. Lokesh, N. Korber, R. M. Gschwind, *Angew. Chem. Int. Ed.* **2019**, *58*, 3133–3137; *Angew. Chem.* **2019**, *131*, 3165–3169.

[17] a) S. Joseph, M. Hamberger, F. Mutzbaurer, O. Härtl, M. Meier, N. Korber, *Angew. Chem. Int. Ed.* **2009**, *48*, 8770–8772; *Angew. Chem.* **2009**, *121*, 8926–8929; b) M. Waibel, F. Kraus, S. Scharfe, B. Wahl, T. F. Fässler, *Angew. Chem. Int. Ed.* **2010**, *49*, 6611–6615; *Angew. Chem.* **2010**, *122*, 6761–6765; c) F. S. Geitner, T. F. Fässler, *Chem. Commun.* **2017**, *53*, 12974–12977.

[18] B. Blom, M. Stoelzel, M. Driess, *Chem. Eur. J.* **2013**, *19*, 40–62.

[19] a) S. S. Sen, M. P. Kritzler-Kosch, S. Nagendran, H. W. Roesky, T. Beck, A. Pal, R. Herbst-Irmer, *Eur. J. Inorg. Chem.* **2010**, 5304–5311; b) S. S. Sen, S. Khan, P. P. Samuel, H. W. Roesky, *Chem. Sci.* **2012**, *3*, 659–682; c) B. Prashanth, S. Singh, *Dalton Trans.* **2016**, *45*, 6079–6087.

[20] a) C.-W. So, H. W. Roesky, J. Magull, R. B. Oswald, *Angew. Chem. Int. Ed.* **2006**, *45*, 3948–3950; *Angew. Chem.* **2006**, *118*, 4052–4054; b) S. Nagendran, S. S. Sen, H. W. Roesky, D. Koley, H. Grubenmüller, A. Pal, R. Herbst-Irmer, *Organometallics* **2008**, *27*, 5459–5463; c) S. S. Sen, H. W. Roesky, D. Stern, J. Henn, D. Stalke, *J. Am. Chem. Soc.* **2010**, *132*, 1123–1126.

[21] a) A. Brück, D. Gallego, W. Wang, E. Irran, M. Driess, J. F. Hartwig, *Angew. Chem. Int. Ed.* **2012**, *51*, 11478–11482; *Angew. Chem.* **2012**, *124*, 11645–11649; b) D. Gallego, A. Brück, E. Irran, F. Meier, M. Kaupp, M. Driess, J. F. Hartwig, *J. Am. Chem. Soc.* **2013**, *135*, 15617–15626; c) B. Blom, D. Gallego, M. Driess, *Inorg. Chem. Front.* **2014**, *1*, 134–148.

[22] a) K. W. Muir, *J. Chem. Soc. A* **1971**, 2663–2666; b) T. D. Tilley, *Organometallics* **1985**, *4*, 1452–1457; c) T. Nguyen, D. Scheschkewitz, *J. Am. Chem. Soc.* **2005**, *127*, 10174–10175.

[23] a) H. G. Woo, R. H. Heyn, T. D. Tilley, *J. Am. Chem. Soc.* **1992**, *114*, 5698–5707; b) A. D. Sadow, T. D. Tilley, *J. Am. Chem. Soc.* **2003**, *125*, 9462–9475; c) C. Kayser, D. Frank, J. Baumgartner, C. Marschner, *J. Organomet. Chem.* **2003**, *667*, 149–153; d) M. Aghazadeh Meshgi, R. Zitz, M. Walewska, J. Baumgartner, C. Marschner, *Organometallics* **2017**, *36*, 1365–1371.

[24] J. Hlina, R. Zitz, H. Wagner, F. Stella, J. Baumgartner, C. Marschner, *Inorg. Chim. Acta* **2014**, *422*, 120–133.

[25] S. Martens, S. Traut, O. Wunnicke, A. Torvisco, R. Fischer, M. Haas, A. Temmel, V. Christopoulos, H. Stueger, *Inorg. Chem.* **2016**, *55*, 4034–4038.

[26] S. P. Mallela, R. A. Geanangel, *Inorg. Chem.* **1990**, *29*, 3525–3528.

[27] J. Baumgartner, R. Fischer, J. Fischer, A. Wallner, C. Marschner, *Organometallics* **2005**, *24*, 6450–6457.

[28] a) W. Yang, H. Fu, J. Wang, M. Chen, Y. Ding, H. W. Roesky, A. Jana, *Inorg. Chem.* **2009**, *48*, 5058–5060; b) B. Blom, S. Enthaler, S. Inoue, E. Irran, M. Driess, *J. Am. Chem. Soc.* **2013**, *135*, 6703–6713; c) M. El Ezzi, T.-G. Kocsor, F. D'Accriscio, D. Madec, S. Mallet-Ladeira, A. Castel, *Organometallics* **2015**, *34*, 571–576; d) J. A. Baus, F. M. Mück, H. Schneider, R. Tacke, *Chem. Eur. J.* **2017**, *23*, 296–303.

[29] a) C. Zybill, G. Müller, *Organometallics* **1988**, *7*, 1368–1372; b) T. A. Schmedake, M. Haaf, B. J. Paradise, A. J. Millevolte, D. R. Powell, R. West, *J. Organomet. Chem.* **2001**, *636*, 17–25.

[30] CCDC 1978002 (**2a**), 1978003 (**2b**), 1978004 (**3a**), 1978005 (**3b**), 1978006 (**3c**), 1978007 (**4a**), 1978008 (**4b**), and 1978009 (**4c**) contain the supplementary crystallographic data for this paper. These data are provided free of charge by The Cambridge Crystallographic Data Centre.

Manuscript received: January 23, 2020
Accepted manuscript online: February 24, 2020
Version of record online: March 20, 2020